Study on Fiber Structure Formation in Wet Spinning of Aliphatic Polyketone Using Aqueous Solution of Complex Metal Salts—Characteristics of Solid Structure Formation in Drying Step and Its Effects on Superdrawing Step

Toru Morita, Ryu Taniguchi, Jinichiro Kato

Asahi Kasei Corporation, R&D Laboratory for Fibers and Textiles Technology, Nobeoka, Miyazaki, 882-0031, Japan

Received 5 September 2003; accepted 31 March 2004
DOI 10.1002/app.20838
Published online in Wiley InterScience (www.interscience.wiley.com).

ABSTRACT: Solid structure formation in the drying step for wet spinning of poly(1-oxotrimethylene) using as a solvent an aqueous solution of complex metal salts of calcium chloride/zinc chloride was studied. Because the degree of structural densification and the crystal structure both differ depending on the drying temperature, the drying temperature had a major effect on the drawing behavior and the strength achieved after drawing. With higher drying temperature, the denseness increased due to smaller voids in the dried undrawn fiber, while there was also a tendency toward higher strength with respect to the draw ratio. However, an excessively high drying temperature altered the crystal structure from a rough crystalline form to a dense crystalline form and reduced both the maximum draw ratio and strength. Mechanical cleavage of the molecular chains occurred between the ethylene groups and carbonyl groups of the main chains in the drawing step. This cleavage made it possible to suppress the inhibition of drawing due to entanglement of the molecular chains, thereby enabling superdrawing to afford a high performance fiber. © 2004 Wiley Periodicals, Inc. J Appl Polym Sci 94: 446–452, 2004

Key words: fibers; strength; structure-property relations

INTRODUCTION

Poly(1-oxotrimethylene) (hereinafter referred to as ECO, Fig. 1), obtained by perfectly alternating copolymerization of ethylene and carbon monoxide, has repeating units and forms a planar zigzag structure.[1] Because of the small sectional area occupied by each polymer chain, ECO can form a high strength, high elastic modulus fiber (ultimate tenacity 266 cN/dtex (34.7 GPa); crystal elastic modulus 2770 cN/dtex (361 GPa)). Because ECO monomers are inexpensive compounds, ECO is expected to come into wide use as a novel industrial material fiber due to its high cost-performance.

The authors discovered that, when ECO is dissolved in an aqueous solution of complex metal salts of calcium chloride/zinc chloride, the solution has a phase-separation temperature at 0°C or above. The authors also discovered a method of producing ECO fiber having high strength and a high elastic modulus comparable to super fiber, which method comprises extruding the solution at above the phase-separation temperature into a coagulation bath at a temperature lower than the phase-separation temperature to form homogeneous gel-like coagulated fiber and then superdrawing it.[2]

More specifically, this wet spinning process is comprised mainly of five steps: 1) dissolving ECO, 2) solidifying it in a coagulation bath, 3) rinsing it to remove the salts, 4) drying it, and 5) superdrawing it. The formation of the fiber structure in the drying step is extremely important in determining the performance of the drawn fiber. If the drying step is not optimized, the superdrawability is not sufficient and the high physical properties therefore cannot be achieved. In this article, we wish to report changes in fiber structure based on the drying conditions and their effect on hot drawing and will further discuss the structure changes during drawing and the features of the physical properties of the drawn fiber.

EXPERIMENTAL

Materials

ECO was synthesized by the following method:[3,4]

A solution of 1.210 g of 1,3-bis[di(2-methoxyphenyl)phosphino]propane in 500 mL of acetone was mixed with a solution of 0.412 g of palladium acetate in 500 mL of acetone. The mixture was stirred for an hour. 4.18 g of trifluoroacetic acid and 39.6 g of *p*-benzoquinone were added to the solution and dissolved.

Correspondence to: J. Kato.

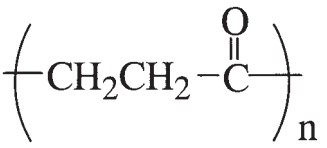

Figure 1 Poly(1-oxotrimethylene) (ECO).

One liter of methanol and 36.5 mL of the prepared catalyst solution were placed in a 2L autoclave, a 1 : 1 mixed gas of ethylene and carbon monoxide was injected therein to a pressure of 5.5 MPa, and the reaction was conducted at 79°C for 4.5 h. After the reaction, the resulting polymer was washed several times with methanol and then dried.

The intrinsic viscosity ([η]) measured in hexafluoroisopropanol at 25°C was 5.5 dL/g.

Spinning method

Wet spinning step (dissolution, coagulation, and washing)

The spinning system is depicted in Figure 2.

ECO was mixed in a calcium chloride/zinc chloride = 40/22 wt % aqueous solution to a concentration of 6.5 wt %, and the mixture was agitated at 80°C for 3 h to obtain a transparent solution (phase-separation temperature: 20°C). Using a plunger extruder A, this solution was extruded from a spinneret B (50 0.15 mm diameter holes) at 80°C through a 10-mm air layer into a coagulation bath C containing 2°C water at a linear velocity of 3 m/min. The coagulated fiber was taken up by a 3 m/min Nelson roll D, then passed through a 0.5 wt % hydrochloric acid bath E, rinsed with rinsing roll F, and the undried fiber G wound up at a speed of 3 m/min.

Drying step

The undried fiber G was pulled up using the system shown in Figure 3 from water bath H using a Nelson roll I, and the fiber was continuously dried at a speed of 1 m/min while bringing it into contact with a hot plate (1 m) J at a predetermined temperature before reaching the Nelson roll K and finally winding up the undrawn fiber L.

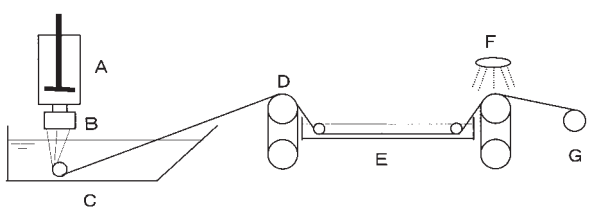

Figure 2 Schematic view of spinning system. A: plunger extruder; B: spinneret; C: coagulation bath; D: takeup roll (Nelson roll); E: 0.5 wt % hydrochloric acid bath; F: rinsing roll (Nelson roll); G: windup (undried fiber).

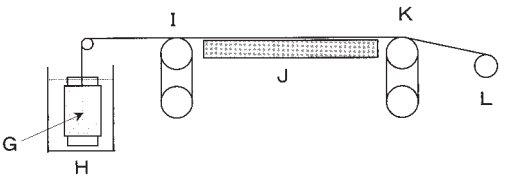

Figure 3 Schematic view of drying system. G: wound-up fiber of Fig. 2; H: water bath; I, K: Nelson roll; J: hot plate; L: windup.

Drawing step

The undrawn fiber L was drawn by the system shown in Figure 4 at different Nelson roll speeds while heating with hot plate (1 m) N at a predetermined temperature.

Observation of cross section of yarn by SEM

The fiber samples were coated with Pt/Pd for 40 s and then observed by a Hitachi S5000 super-high-resolution SEM instrument (Tokyo, Japan) at an accelerating voltage of 1.0 kV.

Measurement of density of fiber

A density gradient tube with carbon tetrachloride and *n*-heptane was used to measure the density of the fiber.

Observation of crystalline form by wide-angle x-ray diffraction patterns

Rigaku Rotaflex RU-200 (Tokyo, Japan) was used under the following conditions:

X-ray source: Ni-filtered CuKα radiation generated at 30 kV and 100 mA, step scans interval: 0.1°.

A fiber-powderized sample was used.

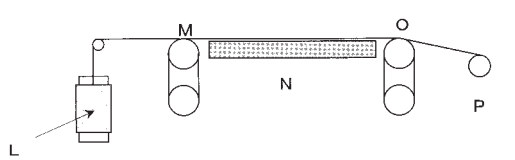

Figure 4 Schematic view of drawing system. L: wound-up fiber (dried fiber or partially drawn fiber); M, O: Nelson roll; N: hot plate; P: windup.

Observation of crystal transition temperature by DSC measurement

Measurements were performed with a Perkin–Elmer DSC Pyris-1 (Wellesley, MA) under flowing nitrogen at a heating rate of 20°C/min.

Observation of lamellae structure by TEM

Undrawn and drawn fibers were cut into small pieces, dyed with a mixed solution of phosphotungstic acid/osmium tetraoxide, and embedded in epoxy resin. The ultrathin sections along the direction of the fiber axis were prepared using an ultramicrotome (LKB2088). The cross section was observed using a Hitachi H-7100 TEM (Tokyo, Japan).

Observation of long-period structure by small-angle x-ray scattering patterns

Fiber bundle samples were used as samples. Measurement was performed with a Rigaku X-ray diffractometer RINT 2000 (Tokyo, Japan) under the following conditions.

X-ray source: Ni-filtered CuKα radiation generated at 40 kV and 152 mA; camera length: 94.5 mm; measurement time: 3 min.

^{1}H-NMR measurement of fiber

^{1}H-NMR spectra were obtained using a Bruker FT-NMR DPX-400 (Bruker BioSpin K. K., Tsukuba, Japan). The samples were dissolved in deuterated hexafluoroisopropanol with deuterated chloroform as an internal standard.

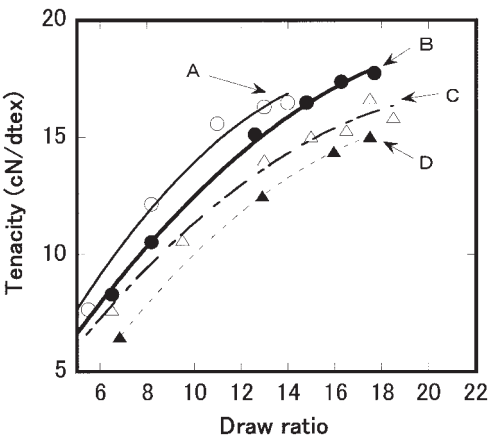

Figure 5 Changes in tenacity with respect to draw ratio at different drying temperatures: A, 250°C; B, 230°C; C, 200°C; and D, 150°C.

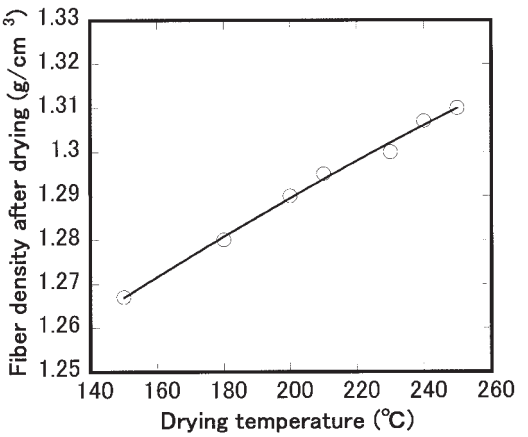

Figure 6 Relationship between fiber density after drying and drying temperature.

RESULTS AND DISCUSSION

Characteristics of solid structure formation in drying step

Figure 5 shows the relationship of the tenacity with respect to the draw ratio when coagulated fibers are dried at different temperatures. Higher drying temperature tended to result in greater strength with respect to the draw ratio. The maximum strength increased with higher drying temperature, but when reaching 250°C, both the drawable ratio and the maximum strength decreased.

Figure 6 shows the density of undrawn fiber after drying at different temperatures. The density of the fiber increased with higher drying temperature. Further, as shown by SEM photograph A of Figure 7, the fiber before drying contained many voids and formed a sponge-like structure, but after drying, the voids in the fiber section fused and disappeared. The extent of this disappearance was also greater as the drying temperature increased, with the cross-sectional structure eventually being altered to a dense structure with no voids. Fiber density is determined by the amount of voids and the crystallinity, but in this case, the amount of voids seems to be the major factor determining the density. The disappearance of voids due to drying occurred because the voids were crushed and fused by the surface tension of the water draining from the voids. Melting point of wet ECO dropped significantly compared to a perfectly dried ECO (Fig. 8). This drop in melting point is believed to be the reason for the ready disappearance of voids due to fusing.

When a fiber with numerous voids is drawn, the voids act as fiber defects and thus inhibit the expression of strength. Therefore, the reduction in maximum strength, despite raising the draw ratio when the drying temperature was low as shown in Figure 5, is attributed to the large amount of voids in the undrawn fiber. Higher drying temperature resulted in smaller

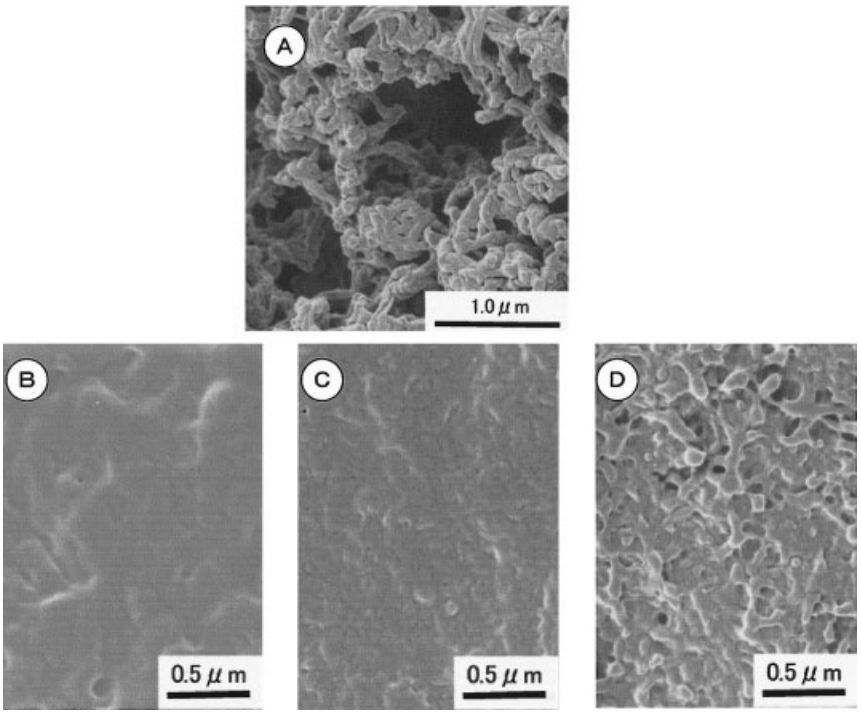

Figure 7 SEM photographs of sectional structure of yarn. (A) fiber before drying (sampling at G of Fig. 2); (B), (C), (D) dried fibers with different drying temperatures (sampling at L of Fig. 3; B: 250°C, C: 230°C, and D: 200°C).

voids and greater density, and consequently a tendency toward higher strength with respect to the same draw ratio.

Figure 9 shows small-angle x-ray scattering patterns and TEM photographs for undrawn fiber dried at 230°C and for fiber drawn at different ratios. In the small-angle x-ray scattering pattern for the undrawn fiber, a ring-shaped long period due to the lamellae crystals was observed. The lamellae crystals of the undrawn fiber were found to be arranged in substantially random directions. In the fiber 3 times drawn, the lamellae crystals were regularly oriented with respect to the fiber axial direction, and the periodic length in the lamellae crystals was larger. In the fiber 16 times drawn, the long-period scattering in the small-angle x-ray scattering pattern disappeared and lamellae crystals were not observed. This shows that a greater draw ratio unfolds the lamellae crystals, thereby increasing the orientation and crystallization of the molecular chains.

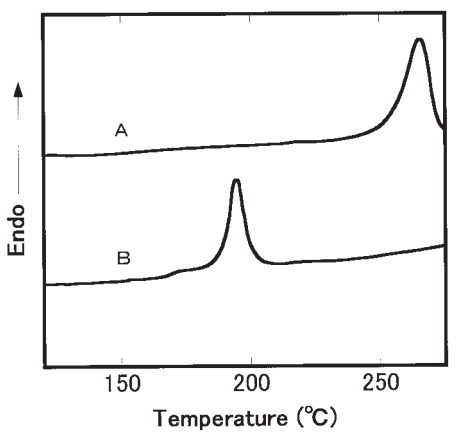

Figure 8 DSC thermograms of ECO. (A) dry ECO; (B) ECO containing 30 wt % water. Both were measured using high pressure-resistant sample pans.

The differences in crystallinity due to the drying temperature is discussed below. Figure 10 shows DSC thermograms of fiber dried at different drying temperatures. No difference was seen in the melting peaks at 250 to 260°C, but a difference in the endothermic peak at 100 to 150°C was apparent and believed to be caused by crystal transition. With a drying temperature of 120°C or 150°C, an endothermic peak (" ↓ "; in the figure) was seen at 140 to 150°C; but with a drying temperature of 200°C or 230°C, no endothermic peak was observed; and with a drying temperature reaching 250°C, an endothermic peak (" ↓ " in the figure) was observed at 110 to 120°C. The endothermic peak observed at 110 to 120°C represents a crystal structure change from the α-form to the β-form.[5] On the other hand, when the drying temperature was 120°C or 150°C, an endothermic peak different from the crystal transition from the α-form to the β-form was observed at 140 to 150°C. As seen in the wide-angle x-ray diffraction patterns shown in Figure 11, when the drying temperature was 120°C or 150°C, a scattering peak

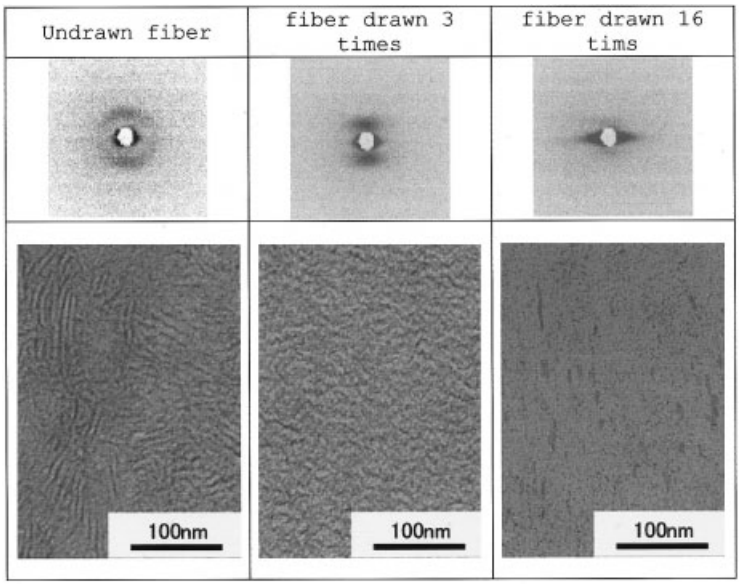

Figure 9 Changes in fiber structure with respect to draw ratio. (Top) small-angle x-ray diffraction patterns; (Bottom) comparisons of TEM photographs.

was observed at the " ↑ " position in the figure, which has not been reported previously.[5] This suggests that the endothermic peak observed at 140 to 150°C is due to the transition from a crystal structure other than the α-form or β-form (here called the "γ-form") to the β-form. When the drying temperature was low, the crystal structure consisted of only γ-form crystals. When the drying temperature was increased, the crystal structure consisted almost entirely of the β-form; and when the drying temperature increased still further, the result was a crystal structure of the α-form. The α-form crystal is denser in structure than the β-form crystal, with a packing energy of -697 J/g for the α-form and -656 J/g for the β-form.[5] Because the drawing involves a step of unfolding the lamellae crystals, a greater proportion of α-form crystals is more resistant to drawing. This is the reason for the drop in the maximum drawing ratio of the undrawn fiber due to drying at 250°C, as shown in Figure 5.

Cleavage of molecular chains by drawing

Table I shows the changes in the intrinsic viscosity ([η]) and changes in the molecular ends as determined by ^{1}H-NMR of the ECO fiber, by drawing 7 times at 230°C of an undrawn fiber, followed by drawing 1.8 times at 260°C, and then by drawing 1.35 times at 270°C. The weight average molecular weights (M_w) in Table I are the values converted from [η] using the Mark–Kuhn–Houwink formula shown below. The co-

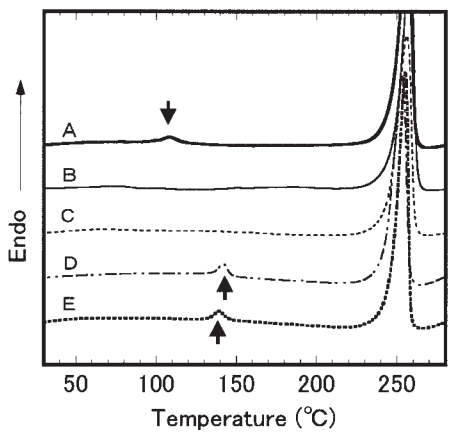

Figure 10 DSC thermograms of fiber dried at different drying temperatures: A, 250°C; B, 230°C; C, 200°C; D, 150°C; and E, 120°C.

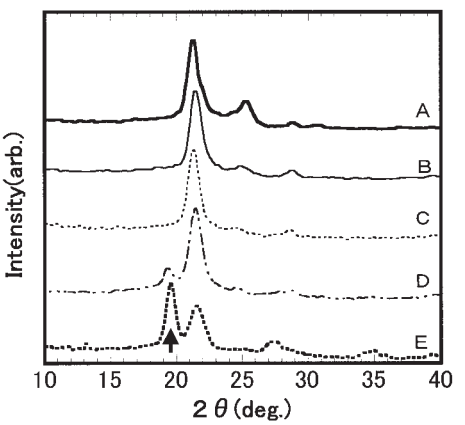

Figure 11 Wide-angle x-ray diffraction patterns of fiber dried at different drying temperatures: A, 250°C; B, 230°C; C, 200°C; D, 150°C; and E, 120°C.

TABLE I
Changes in Molecular Weight and Molecular End Groups of ECO Fiber After Drawing

	Undrawn fiber	Drawn fiber		
		7X	12.6X	17X
[η] (dL/g)	5.5	3.7	3.3	3.1
Mw (converted from [η])	252,000	148,000	127,000	117,000
^{1}H-NMR peak area ratio				
–C$\underline{H}_2$C$\underline{H}_2$CO (main chain)	1	1	1	1
–C(O) $CH_2C\underline{H}_3$ (end group)	0.00036	0.00061	0.00072	0.00076
–COOC$\underline{H}_3$ (end group)	0.00032	0.00034	0.00033	0.00032
M_n (from ^{1}H-NMR data)	124,000	88,000	80,000	78,000
M_w/M_n	2.03	1.68	1.59	1.50

efficient in the Mark–Kuhn–Houwink formula was determined by preparing ECO with different [η] values and measuring the M_w by the GPC-LALLS method using hexafluoroisopropanol as the solvent.

$$[\eta] = 5.2 \times 10^{-4} \times M_w^{0.745} \quad (1)$$

The molecular weight was lower with a higher draw ratio.

The molecular chain cleavage during drawing based on changes in the end groups found by ^{1}H-NMR measurement was evaluated. The end groups of the ECO are -$COOCH_3$ and -$C(O)CH_2CH_3$ derived from the polymerization solvent (methanol).[6] Based on the ratios of the peak areas of the methyl protons of -$COOCH_3$ and -$C(O)CH_2CH_3$ each with respect to the peak area of the ethylene protons of the main chain, it was found that the ratio of the -$COOCH_3$ groups did not change significantly but that the ratio of -$C(O)CH_2CH_3$ increased in correspondence with the reduction in [η]. Molecular cleavage is thought to occur between the ethylene groups and carbonyl groups of the main chain, thereby producing more -$C(O)CH_2CH_3$ groups, as shown in the scheme of Figure 12. The end groups produced by this molecular cleavage are believed to be aldehyde groups or vinyl groups, etc., but at the present time, this has not been clearly observed by ^{1}H-NMR or ^{13}C-NMR analysis.

The fact that the molecular weight distribution (M_w/M_n) gradually narrowed due to drawing along

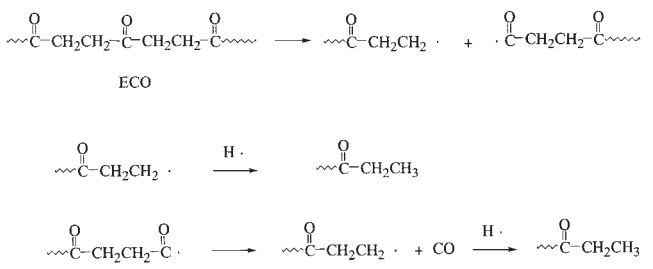

Figure 12 Scheme of mechanical molecular cleavage in drawing step.

with the rise in the draw ratio (Table I) and the fact that almost no drop in molecular weight was observed by heating at the same time as drawing suggest that the molecular cleavage of ECO during drawing was mechanical cleavage, wherein the high molecular weight chains that easily entangle were cleaved preferentially. Such molecular cleavage during hot drawing suppressed the inhibition of drawing that is due to the entanglement of molecular chains, so that drawing and orientation could proceed more smoothly and superdrawing by as much as 17 times becomes possible.

Features of ECO fiber after drawing

As shown above, drawing of ECO caused the lamellae crystals to become unfolded while the molecular chains gradually became oriented and crystallization proceeded, resulting in a high strength, high elastic modulus fiber on par with super fiber, as shown in Figure 13. Further, because the drawn fiber of ECO had a high degree of orientation and crystallinity, it was characterized by superior dimensional stability at

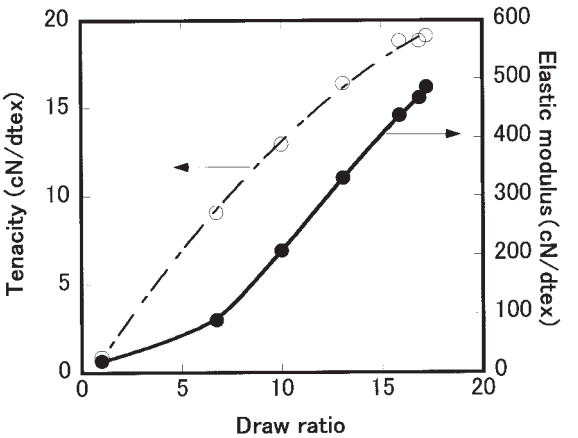

Figure 13 Changes in tenacity and elastic modulus of ECO fiber with respect to draw ratio (drying temperature is 230°C).

high temperature and high temperature retention ratio of elastic modulus compared with organic fiber having substantially the same melting point, such as PET (polyethylene terephthalate) fiber.

The heat shrinkage shown in Table II is the length change before and after heat treatment at 160°C for 30 min. If treated at a temperature above the glass transition temperature, the oriented molecular chains relax at the amorphous regions so that large fiber shrinkage occurs. ECO fiber has a higher degree of crystallinity compared with PET fiber, so presumably there is little effect due to relaxation of the molecular chains at the amorphous sections and the heat shrinkage is minimal.

Figure 14 shows the storage elastic modulus with measurement of the dynamic viscosity while raising the temperature. Here, the storage elastic modulus of the PET fiber decreased rapidly when the temperature was higher than the glass transition temperature. On the other hand, the storage elastic modulus of ECO fiber was high and almost flat at 0–200°C. The small change at 110 to 120°C (" ↑ " in the figure) is attributed to the crystal transition from the α-form to the β-form.

CONCLUSION

The drying step is an important structure-forming step determining the superdrawability, based on the fact that the density and crystalline form change depending on the drying temperature for spinning of ECO when using an aqueous solution of complex metal salts of calcium chloride/zinc chloride as the solvent. A higher drying temperature resulted in smaller voids and denser undrawn fiber after drying, as well as a higher strength with respect to the draw ratio and a higher maximum strength. It was also found, however, that if the drying temperature was too high, the crystal structure changed from a rough crystalline form to a dense crystalline form, the lamellae crystals became harder to unfold, and both the maximum drawing ratio and maximum strength were reduced.

TABLE II
Melting Point and Heat Shrinkage of ECO Fiber and PET Fiber

	ECO fiber	PET fiber
Melting point (°C)	270	260
Heat shrinkage (%)	0.5	4.0

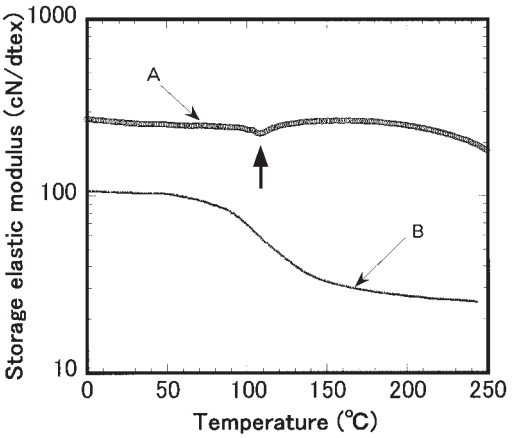

Figure 14 Temperature dependency of storage elastic modulus: A, ECO fiber; B, PET fiber.

For unfolding of the lamellae crystals to obtain highly oriented molecular chains in the drawing step, mechanical cleavage of the molecular chains occurred between the ethylene groups and carbonyl groups of the main chains. This molecular cleavage during drawing suppressed the inhibition of drawing that occurred due to entanglement of the molecular chains, thus facilitating drawing and orientation and enabling superdrawing.

ECO fibers with highly oriented molecular chains and highly crystalline structures were characterized not only by a higher level of strength and elastic modulus but also by superior dimensional stability at high temperature and high temperature retention ratio of the elastic modulus compared with organic fiber having substantially the same melting point, such as PET fiber. This is because ECO fibers are highly crystallized and contain few amorphous regions and the surrounding crystals constrain movement of the molecular chains at the amorphous regions.

References

1. Lommerts, B. J.; Klop, E. A.; Aerts, J. J Polym Sci Part B: Polym Phys 1993, 31, 1319.
2. Kato, J.; Morita, T.; Taniguchi, R. PCT W002/068738, 2002.
3. Broekhoven, J. A. M. v.; Wife, R. L. E P Appl 1987, 257, 663.
4. Broekhoven, J. A. M. v.; Miedema, W. E P Appl 1989, 360, 359.
5. Klop, E. A.; Lommerts, B. J.; Vaurink, J.; van Puijenbroek, R. R. J Polym Sci Part B: Polym Phys 1995, 33, 315.
6. Drent, E.; Budzelaar, P. H. M. Chem Rev 1996, 96, 663.